Inhibition of Human Leukocyte and Porcine Pancreatic Elastase by Homologues of Bovine Pancreatic Trypsin Inhibitor†

James A. E. Kraunsoe, Timothy D. W. Claridge, and Gordon Lowe*

Dyson Perrins Laboratory and Oxford Centre for Molecular Sciences, Oxford University, South Parks Road, Oxford OX1 3QY, U.K.

Received December 20, 1995; Revised Manuscript Received April 24, 1996⊗

ABSTRACT: The interactions of three BPTI homologues with human leukocyte elastase and porcine pancreatic elastase have been investigated. The principal mutation in determining the specificity of inhibition was the Lys[15]-Val mutation at the P_1 position. An additional mutation at P_3, i.e., BPTI (Lys[15]-Val, Pro[13]-Ile), increased the inhibition of HLE to a $K_i = 2.5 \times 10^{-10}$ M, but decreased the inhibition of PPE, showing this to be a useful site for improving selectivity. Kinetic evidence suggests that the inhibition of HLE by BPTI homologues probably takes place by a two-step mechanism in which an isomerization step occurs after initial binding. ^{1}H NMR spectroscopy of the BPTI (Lys[15]-Val) and BPTI (Lys[15]-Val, Pro[13]-Ile) mutants indicates that small conformational changes are associated with the mutations, but these are localized in the immediate vicinity of the mutation in the outer binding loop and in the inner loop connected to it through the Cys[14]−Cys[38] disulfide bridge.

A large number of protein proteinase inhibitors have been characterized, and are currently attracting considerable attention. This arises because of their importance in regulating the activity of their target proteinases but also because the availability of high-resolution structural data makes them suitable models for the study of protein−protein interactions (Bode & Huber, 1992, 1994; Tschesche, 1974).

The majority of protein proteinase inhibitors known and characterized so far are inhibitors of serine proteinases. There are at least 18 different families, and for 12 of these, the tertiary structure of at least 1 representative is known (Bode & Huber, 1994). Bovine pancreatic tryptin inhibitor (BPTI)[1] is one of the most thoroughly studied of these proteinase inhibitors, not only for its anti-proteinase activity (Fritz & Wunderer, 1983), but also for the work carried out in elucidating the pathways of protein folding (Creighton, 1992; Staley & Kim, 1990).

BPTI is a highly stable, basic protein consisting of a single polypeptide chain of 58 amino acids. The polypeptide chain is cross-linked by three-disulfide bridges which, in part, account for its high stability to denaturation (Kassel, 1970). The structure of BPTI has been solved using X-ray diffraction (Deisenhofer & Steigmann, 1975; Wlodawer et al., 1987), joint refinement with X-ray and neutron diffraction (Wlodawer et al., 1984), NMR spectroscopy in solution (Berndt et al., 1992; Wagner et al., 1987), and simultaneous refinement of X-ray diffraction data in single crystals with NMR data in solution (Schiffer et al., 1994).

The crystal structures of the BPTI complexes with β-trypsin and porcine kallikrein A have also been solved (Chen & Bode, 1983; Huber et al., 1974). These have shown that the region of interaction, as for many other proteinase inhibitors, is between the active site cleft of the proteinase and an external loop region of the BPTI. The binding loop is held in a rather rigid conformation by its interaction with a secondary loop and with the core of the molecule. The complementarity of the loop region and the number of interactions made between the loop and trypsin are responsible for the high binding energy and the very low inhibition constant, $K_i = 6 \times 10^{-14}$ M (Lazdunski & Vincent, 1972).

As part of a program to generate effective inhibitors toward clinically important proteinases and to understand the nature of the interactions between proteinase inhibitors and proteinases, BPTI has been modified in its inhibitory loop. In this report, we describe the kinetic analysis of BPTI homologues in which residues in the native BPTI sequence have been substituted by amino acids found in the inhibitory loop of α_1-proteinase inhibitor (α_1-PI). α_1-PI is a major inhibitor of circulatory serine proteinases (Lobermann et al., 1984). Its principal target *in vivo* is human leukocyte elastase (HLE) (Lomas et al., 1993), whose normal role is phagocytosis and the defence against microbial infection (Bode et al., 1989). As with other elastases, HLE is capable of destroying many connective tissue proteins (Carrell et al., 1982), and its uncontrolled activity has been linked to a variety of disease states including pulmonary emphysema and rheumatoid arthritis (Tetley, 1993).

BPTI, which has been clinically characterized in its native form (Davis & Whittington, 1995; Verstraete, 1985), represents an excellent model for therapeutic targeting in a modified form. Thus, by mutagenesis it is possible to investigate which features are important for the specificity and the inhibitory activity of BPTI homologues.

The BPTI homologues discussed in this paper have been obtained by recombinant DNA technology and characterized by HPLC, electrospray mass spectrometry, and N-terminal sequencing (Chesshyre et al., 1995). BPTI (Lys[15]-Val) has also been produced semisynthetically and its dissociation

† This work was supported by the EPSRC and the BBSRC.

⊗ Abstract published in *Advance ACS Abstracts,* June 15, 1996.

[1] Abbreviations: BPTI, bovine pancreatic trypsin inhibitor; HLE, human leukocyte elastase; PPE, porcine pancreatic elastase; L-BAPNA, N_α-benzoyl-L-arginine *p*-nitroanilide; ESIV, elastase substrate IV (succinyl-Ala-Ala-Pro-Abu *p*-nitroanilide, Calbiochem); ESI, elastase substrate I (MeO-succinyl-Ala-Ala-Pro-Val *p*-nitroanilide, Calbiochem); TOCSY, total correlation spectroscopy.

S0006-2960(95)03013-3 CCC: $12.00

constants with PPE and HLE determined (Beckmann et al., 1988). The K_i values obtained for semisynthetic BPTI (Lys[15]-Val) with PPE and HLE were 5.7×10^{-8} M and 1.1×10^{-10} M, respectively, but k_{on} and k_{off} were not determined, nor were the exact experimental conditions presented.

MATERIALS AND METHODS

Bovine pancreatic trypsin (Sigma; type XIII) was assayed in 0.25 M Tris·HCl, pH 8.0, with 10 mM $CaCl_2$ at 25 °C, with the substrate N_α-benzoyl-L-arginine *p*-nitroanilide (L-BAPNA). Trypsin concentrations were determined by active site titration with *p*-nitrophenyl *p*′-guanidinobenzoate (Chase & Shaw, 1967). Subsequently, values of k_{cat} and K_m for trypsin with L-BAPNA were used to calculate enzyme concentrations from initial rates. Porcine pancreatic elastase (PPE; Sigma; type IV) was assayed in 0.2 M Tris·HCl, pH 8.0, at 25 °C with succinyl-Ala-Ala-Pro-Abu *p*-nitroanilide (ESIV; elastase substrate IV; Calbiochem) as substrate. Enzyme concentrations were determined from initial rates with values of $k_{cat} = 10.2\ s^{-1}$ and $K_m = 0.03$ M (Largman, 1983). Human leukocyte elastase (HLE; Sigma) was assayed in 0.1 M HEPES, pH 7.5, with 0.5 M NaCl and 9.8% DMSO and 1% v/v 10 mg/mL BSA (Sigma; fraction V) at 25 °C with MeO-succinyl-Ala-Ala-Pro-Val *p*-nitroanilide (ESI; elastase substrate I; Calbiochem) as substrate. Enzyme concentrations were determined from initial rates with values of $k_{cat} = 17\ s^{-1}$ and $K_m = 0.14$ mM (Nakajima et al., 1979).

Inhibitor concentrations were determined from stoichiometric binding curves with PPE or HLE and correlated with A_{214nm} and A_{280nm} values. A solution of BPTI of 1 mg/mL has $A_{214nm} = 19.7$ and $A_{280nm} = 0.84$ (Fritz & Wunderer, 1983). Active site concentrations were determined as indicated above. The actual values were 34% of the theoretical maximum for PPE and 48% for HLE.

Slow-Binding Kinetics. Inhibitors were investigated using the slow-binding procedure (Cha, 1975; Morrison & Walsh, 1988). Inhibitors were treated as slow-binding if the attainment of the steady-state could be observed over a period of minutes and the data could be successfully fitted to the slow-binding eq 1. For the simplest treatment of slow-binding data, experiments were carried out under pseudo-first-order conditions where the lowest [I] ≥ 10[E]. The enzyme concentration was set at a suitably low level so as to give a measurable rate of substrate hydrolysis as well as an observable rate of inhibitor binding over the steady-state time scale. The initial concentration of substrate was sufficiently high to allow the reaction to be followed for an adequate time, but with less than 10% of the substrate being hydrolyzed by the end of the experiment. Reactions were carried out under the same conditions as described above. PPE concentrations were approximately 0.25 nM or 0.5 nM. Inhibitor concentrations [BPTI (Lys[15]-Val)] were between 0 and 240 nM. Substrate concentration was 0.8 mM. HLE concentrations were 1 nM or 0.5 nM. Inhibitor concentrations were between 0 and 120 nM [BPTI (Lys[15]-Val)], 0 and 18.3 nM [BPTI (Lys[15]-Val, Pro[13]-Ile)], and 0 and 90.7 nM [BPTI (Lys[15]-Val, Gly[12]-Ala)]. The substrate concentration was 0.845 nM. Six cuvettes (0.7 mL) were incubated at 25 °C in a Cary 3/E UV/Vis double-beam spectrophotometer fitted with an automatic cell changer (2 × 6 cells). Reactions were stirred during the course of the experiment using 3 mm magnetic bars. Cells containing buffer were used as blanks. An independent experiment showed the change in concentration of ESIV and ESI to be negligible over the course of a typical slow-binding experiment (8 h). Reactions were initiated by the addition of the enzyme (70 μL) preequilibrated at 20 °C. Data were collected every 30 s during the course of the experiment (between 2 and 8 h). On completion of the experiment, all the data were transferred to KaleidaGraph, zeroed, and analyzed using nonlinear regression analysis.

Data Analysis (Longstaff et al., 1990). Data from each curve at different inhibitor concentrations were fitted to eq 1, the integrated rate equation describing substrate hydrolysis in the presence of a slow-binding inhibitor:

$$A = V_s t + (V_0 - V_s)(1 - e^{-k't})/k' + A_0 \qquad (1)$$

A = the absorbance at 410 nm, A_0 = the initial absorbance, V_0 = the initial rate, V_s = the final steady-state rate, and k' = the apparent first-order rate constant for the transition to the steady-state.

For the simplest model of complex formation, E + I = EI, a plot of k' vs [I] gives a straight line from which k_{on} and k_{off} can be determined according to eq 2:

$$k' = k_{off} + k_{on}[I]/(1 + [S]/K_m) \qquad (2)$$

A plot of $(V_0 - V_s)/V_s$ against [I] can be used to determine K_i and should give a straight line passing through the origin according to eq 3:

$$(V_0 - V_s)/V_s = [I]/\{K_i(1 + [S]/K_m)\} \qquad (3)$$

Where V_0 could not be determined accurately from fitting, eq 2 was not used. Equation 3 could still be used to calculate K_i, but V_i, the uninhibited enzyme rate, was used instead of V_0.

Dissociation Kinetics. Direct determination of the dissociation rate constant (k_{off}) may be made by diluting preformed enzyme−inhibitor complex into concentrated substrate solution. For this to be successful, stoichiometric binding should be observed, and the complex should be diluted below its apparent K_i [$K_{i(app)} = K_i\{1 + [S]/K_m\}$]. The rate equation for complex dissociation is given in eq 4:

$$[E] = [E_0](1 - e^{-k_{off}t}) \qquad (4)$$

Data were fitted to the integrated form, eq 5. $[E_0]$ was determined from the final steady-state rate after complex dissociation. k_{off} for PPE with BPTI (Lys[15]-Val) and BPTI (Lys[15]-Val, Pro[13]-Ile) was determined in this way by diluting the complex (70 μL) into 0.8 mM buffered substrate (ESI; 0.63 mL). Release of free enzyme was monitored by substrate hydrolysis on a Cary 3/E UV/Vis double-beam spectrophotometer. KaleidaGraph was used to fit the data to eq 5 by nonlinear regression analysis:

$$A = \{k_{cat}[E_0](k_{off}t + e^{-k_{off}t} - 1) + A_0\}/k_{off} \qquad (5)$$

NMR Spectroscopy. Wild-type BPTI and the (Lys[15]-Val) and (Lys[15]-Val, Pro[13]-Ile) mutants were studied as ca. 3 mM solutions in unbuffered 90% H_2O/10%D_2O at pH 4.6. Insufficient BPTI (Lys[15]-Val, Gly[12]-Ala) was available for NMR spectroscopic investigation. Spectra were recorded at probe temperatures of 309 K on a Bruker AMX500 spec-

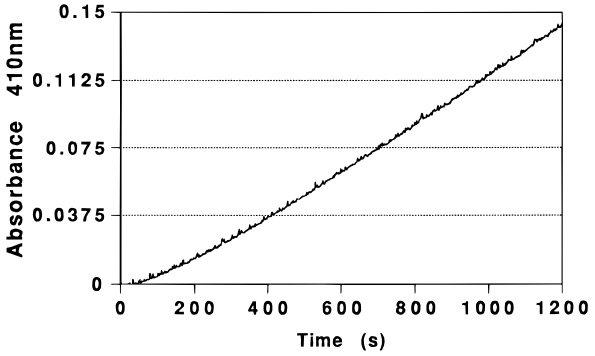

FIGURE 1: Dissociation of BPTI (Lys[15]-Val, Pro[13]-Ile)−PPE complex. The preformed complex was diluted (final concentration 0.5−1.0 nM) into substrate solution (0.8 mM) and complex dissociation followed by monitoring substrate hydrolysis on release of enzyme at 25 °C in 0.2 M Tris·HCl buffer, pH 8.0. Data were fitted to eq 5 as described under Materials and Methods for the direct determination of the dissociation rate constant, k_{off}.

trometer equipped with an inverse $^1H/^{13}C$ probe. Chemical shift assignments were taken from cross-peaks observed in 2D TOCSY (total correlation spectroscopy) spectra (Braunschweiler & Ernst, 1983, Bax & Davis, 1985). These were recorded with the DIPSI-2 isotropic mixing scheme (Rucker & Shaka, 1989) using a B_1 field strength of 8.6 kHz and a z-filter sequence to produce pure-phase spectra (Rance, 1987). Spin-lock mixing periods of 33 and 53 ms were used, and solvent suppression was achieved via presaturation. Quadrature detection was via time-proportional phase incrementations (TPPI), and flat baseplanes were obtained in the resulting spectra by suitable adjustment of the receiver (Hoult et al., 1983; Marion & Bax, 1988). Typically, 2K real data points were collected for each of 512 t_1 increments of 40 scans. Data were processed with shifted sine-bell squared window functions in both dimensions, and a polynomial base-line correction was applied in F_2 to correct small residual base-line distortions. Spectra were referenced to 3-(trimethylsilyl)propionate (TSP). Assignments for the wild-type BPTI were taken from Wagner et al. (1987).

RESULTS

Inhibition of PPE by BPTI (Lys[15]-Val), BPTI (Lys[15]-Val, Pro[13]-Ile), and BPTI (Lys[15]-Val, Gly[12]-Ala). Initially, the slow-binding kinetic approach was used to investigate the interaction between BPTI (Lys[15]-Val) and PPE. However, the equilibrium between the enzyme and the inhibitor is rapidly achieved, and BPTI (Lys[15]-Val) behaves as a classical reversible inhibitor. k' and V_0 could not be determined, but V_s could be fitted accurately and K_i was determined from eq 3 using V_i, the uninhibited rate, and V_s. The K_i was determined at two enzyme concentrations to be 3 ($\pm$1) $\times$ 10^{-8} M. Due to the scarcity of recombinant BPTI (Lys[15]-Val, Pro[13]-Ile) and BPTI (Lys[15]-Val, Gly[12]-Ala), the K_i values were not determined, although it was shown in preliminary experiments that the inhibition of PPE followed classical and not slow-binding inhibition.

Preformed complexes of PPE with BPTI (Lys[15]-Val), BPTI (Lys[15]-Val, Pro[13]-Ile), and BPTI (Lys[15]-Val, Gly[12]-Ala) were dissociated by dilution into concentrated substrate solution. Results from one such experiment, for BPTI (Lys[15]-Val, Pro[13]-Ile), are shown in Figure 1. There is a short lag phase while complex dissociation occurs and before a steady-state of enzyme activity is reached. The data were fitted to eq 5,

Table 1: Summary of Kinetic Constants between PPE and the Anti-Elastase BPTI Mutants

BPTI homologue	k_{on} (M^{-1} s^{-1})	k_{off} (s^{-1})	K_i (M)
BPTI (Lys[15]-Val)	1.7×10^{5} [a]	4.8×10^{-3}	3×10^{-8}
BPTI (Lys[15]-Val, Pro[13]-Ile)	ND[b]	7.3×10^{-3}	ND[b]
BPTI (Lys[15]-Val, Gly[12]-Ala)	ND[b]	$>10^{-2}$	ND[b]

[a] k_{on} was determined from K_i and k_{off} by use of the relationship $K_i = k_{off}/k_{on}$. [b] Not determined.

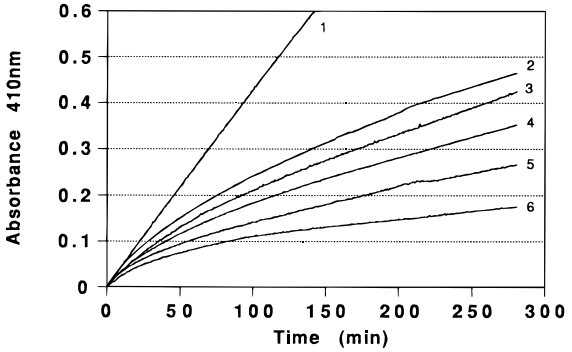

FIGURE 2: Family of slow-binding curves for HLE and BPTI (Lys[15]-Val). Each curve shows the course of enzyme inhibition at a different inhibitor concentration, and the line represents uninhibited enzyme. Data were collected for a total time of 8 h at 25 °C in 0.1 M HEPES buffer containing 0.5 M NaCl, 9.8% DMSO, and 1% v/v 10 mg/mL BSA. Enzyme concentration was approximately 0.5 nM, substrate concentration was 0.845 mM, and inhibitor concentrations were 0, 40.9, 57.4, 73.5, 88.9, and 106.3 nM (curves 1−6, respectively). Reactions were initiated by the addition of an enzyme solution (70 μL) to inhibitor and substrate (0.63 mL).

and k_{off} was determined directly from this analysis. Results from these experiments gave k_{off} for BPTI (Lys[15]-Val) as 4.8 ($\pm$0.1) $\times$ 10^{-3} s^{-1} and for BPTI (Lys[15]-Val, Pro[13]-Ile) as 7.3 $\times$ 10^{-3} s^{-1}. Attempts to measure k_{off} for PPE and BPTI (Lys[15]-Val, Gly[12]-Ala) were unsuccessful, as complete dissociation occurred before data collection could start (i.e., within 30 s). As a result, k_{off} was estimated to be not less than 10^{-2} s^{-1}. All the constants determined for the inhibition of PPE are given in Table 1.

Inhibition of HLE by BPTI (Lys[15]-Val), BPTI (Lys[15]-Val, Pro[13]-Ile), and BPTI (Lys[15]-Val, Gly[12]-Ala). All three BPTI homologues were shown to be slow-binding inhibitors of HLE. A family of binding curves for the inhibition by BPTI (Lys[15]-Val) is shown in Figure 2. Data from this experiment, and similar experiments for BPTI (Lys[15]-Val, Pro[13]-Ile) and BPTI (Lys[15]-Val, Gly[12]-Ala), were fitted to eq 1 by nonlinear regression analysis as described under Materials and Methods. The values determined for k', V_0, and V_s were used to plot graphs from which k_{on} and K_i were determined, for example, Figure 3. Figure 3a is a plot of k' vs [I], the slope of which can be used to calculate k_{on}. Theoretically, k_{off} can be determined from the intercept on the *y* axis, but in practice, this is very close to zero, and therefore small variations in the gradient can lead to a large variation in the value for k_{off}. k_{off} was determined from V_0 and V_s using eq 3 and is demonstrated in Figure 3b.

The data in Figure 2 show that the rate of substrate hydrolysis declines exponentially in the presence of BPTI (Lys[15]-Val) from an initial rate to a final steady-state rate, but does not reach zero even in the presence of a 200-fold molar excess. Two kinetic mechanisms are consistent with such progress curves: (i) the reactions of the enzyme and the inhibitor are reversible, and therefore some free enzyme

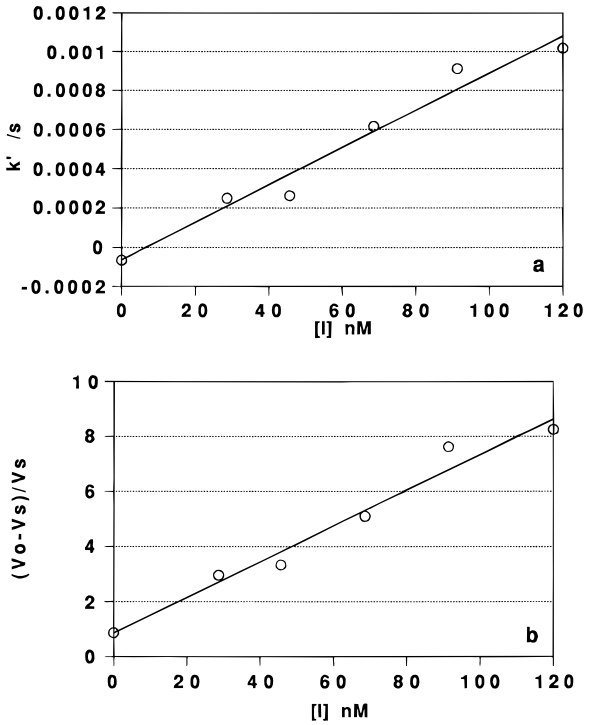

FIGURE 3: Analysis of data for HLE and BPTI (Lys[15]-Val). (a) Plot of k' determined at each inhibitor concentration by fitting data from Figure 2 to eq 1. (b) Determination of K_i using values of V_0 and V_s generated from eq 1.

always exists; or (ii) the irreversible inhibited enzyme retains residual activity. The data in Figure 2 showing the effect of BPTI (Lys[15]-Val) concentration on the progress curves are only compatible with (i) as this shows that the steady-state rate decreases with increasing inhibitor concentration, when the enzyme concentration is held constant. For (ii), the steady-state rate (or residual activity) would vary only with the enzyme concentration. Thus, the reaction is reversible with respect to the recovery of the active enzyme. Due to the small amounts of recombinant BPTI homologues, it was not possible to recover the inhibitor and confirm that it was released in an active form.

Kinetic Mechanism. The original analysis of slow-binding inhibitors (Cha, 1975) [for a review, see Morrison and Walsh (1988) proposes four mechanisms for reversible enzyme inhibition, which produce progress curves described by eq 1. The two most likely mechanisms are shown in Scheme 1.

Mechanism A represents the simple bimolecular association of an enzyme and inhibitor in which complex association occurs rapidly and in one step. k_{on} will therefore reflect the rate at which the molecules encounter each other in solution (modified by a steric factor) and will approach the diffusion-controlled limit, i.e., 10^6-10^8 M^{-1} s^{-1}. For mechanism B, the initial enzyme−inhibitor complex (E·I) undergoes a slow isomerization step to produce a tight, but still dissociable, complex (E·I*). The manifestation of this mechanism in the progress curves of hydrolysis is that the initial rate, V_0, decreases with increasing inhibitor concentration. This mechanism also predicts that the value of k' should increase with inhibitor concentration (Cha, 1975). Evidence supporting mechanism B for the inhibition of HLE by the BPTI homologues is provided by (a) the values for k_{on}, which are several orders of magnitude lower than the diffusion-controlled limit, and (b) the initial rate, V_0, which was shown

Scheme 1: Mechanisms for Reversible Slow-Binding Inhibition

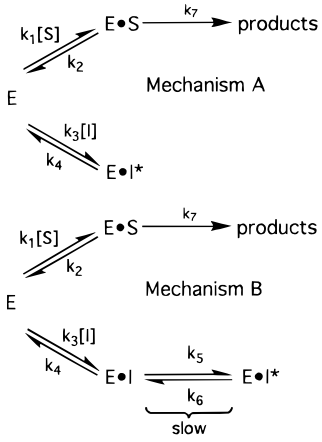

Table 2: Summary of Kinetic Constants between HLE and BPTI (Lys[15]-Val), BPTI (Lys[15]-Val, Pro[13]-Ile), and BPTI (Lys[15]-Val, Gly[12]-Ala)

BPTI homologue	k_{on} (M^{-1} s^{-1})	k_{off} (s^{-1})[a]	K_i (M)
BPTI (Lys[15]-Val)	$5.4\ (\pm1) \times 10^4$	1.5×10^{-4}	$2.8\ (\pm1) \times 10^{-9}$
BPTI (Lys[15]-Val, Pro[13]-Ile)	$8.6\ (\pm1) \times 10^4$	2.2×10^{-5}	$2.5\ (\pm1) \times 10^{-10}$
BPTI (Lys[15]-Val, Gly[12]-Ala)	$2.1\ (\pm0.1) \times 10^4$	7.4×10^{-4}	$3.5\ (\pm1) \times 10^{-8}$

[a] k_{off} was determined from K_i and k_{on} by use of the relationship $K_i = k_{off}/k_{on}$.

to decrease with increasing inhibitor concentrations. However, plots of k' vs [I] did not show the expected hyperbolic deviation from linearity as [I] increased. It is possible that over the range of inhibitor concentration employed for the three BPTI homologues, a sufficiently high [I] was not reached for this to have been observed. All the constants determined for the inhibition of HLE are given in Table 2.

Inhibition of Trypsin. None of the three BPTI homologues inhibit trypsin (data not shown).

Comparison of the ^{1}H TOCSY NMR Spectra of BPTI (Lys[15]-Val) and BPTI (Lys[15]-Val, Pro[13]-Ile) with Wild-Type BPTI. BPTI has been extensively studied by NMR spectroscopy and its three-dimensional structure in solution determined from NMR derived constraints (Wagner et al., 1987). In this present work, it is desirable to know to what extent the conformation of the protein has been disrupted by the mutations, particularly in the region of the binding loop. This could, in principle, be obtained by determining the solution structure of each mutant by NMR spectroscopy. However, data for the wild-type protein have shown the loop region to be poorly defined in NMR studies, notably due to a lack of NOE constraints in this region, and it therefore seems unlikely that any detailed structural data could be obtained for the mutants. Fortunately, the chemical shifts of protons, particularly amide protons, in the protein reflect conformational preferences and are sensitive to conformational changes. We have made a study of these shifts, in comparison with shifts of the wild-type protein, in order to assess the extent of conformational change caused by modifications in the sequence.

Discernible chemical shift differences ($\geq$0.01 ppm) between the amide proton shifts for the wild-type protein and the mutants are presented in Figure 4. For the BPTI (Lys[15]-Val) mutant, the largest differences are observed for the

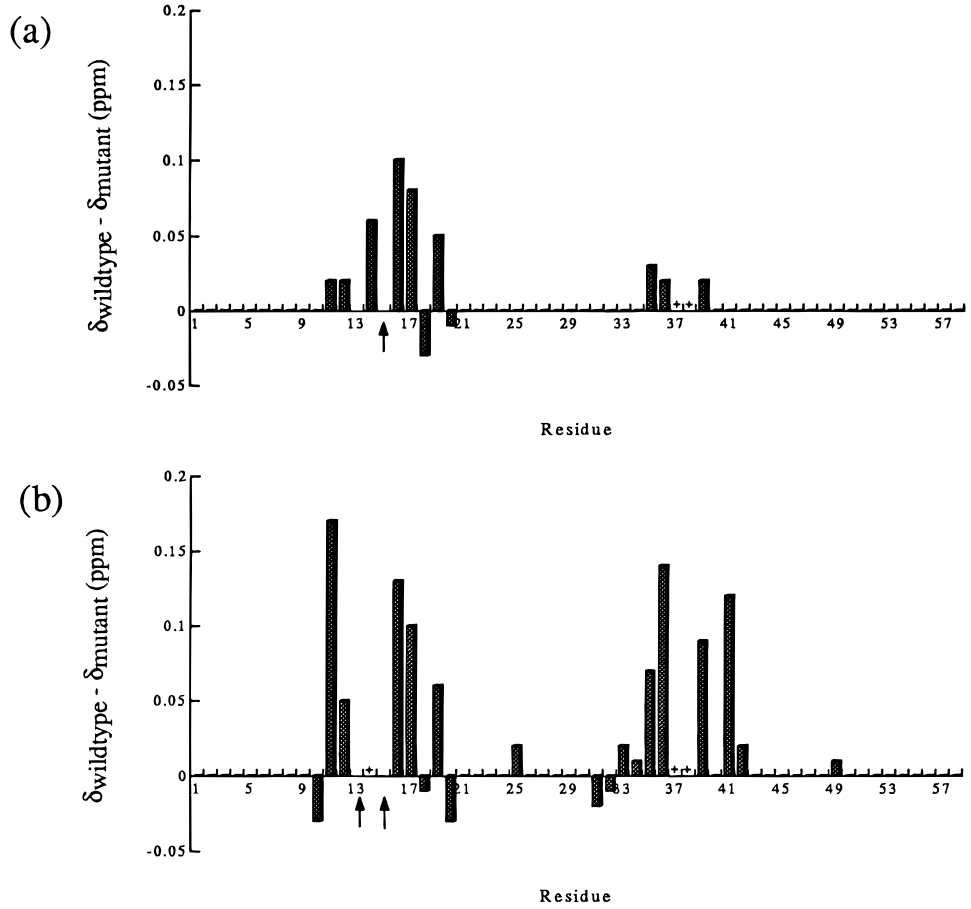

FIGURE 4: Amide NH shift differences (in ppm) from wild-type BPTI for (a) BPTI (Lys[15]-Val) and (b) BPTI (Lys[15]-Val, Pro[13]-Ile). An arrow indicates a position of mutation, and + indicates that the NH shift could not be determined. No NH shift difference is observed for position 13 since this is Pro in wild-type BPTI. The NH shift difference for residue 15 in (a) is 0.47 ppm and in (b) is 0.38 ppm. These are not included in (a) and (b) because they reflect the chemical as well as structural change and should not be regarded as a measure of the conformational change.

residues adjacent to position 15 (14−19), with smaller effects transmitted out to residues 11 and 20 (Figure 4a). It is also interesting to note that small differences were observed for residues 35−39 which correspond to the "inner-loop" of the binding region. In all cases, the magnitude of the differences is no greater than 0.1 ppm. except for that at position 15 which is expected to arise from a combination of chemical and conformational changes and for this reason is not shown in Figure 4a (see legend). The amide shift of residue Cys[38] could not be observed as the C_α proton was coincident with the position of H_2O and relayed correlations to C_β protons were also not seen. The amide proton of Gly[37] is not observed for the wild type (Wagner et al. 1987) or the mutant protein. Shift differences for the $C_\alpha H$ protons (not shown) were no greater than 0.01 ppm for all residues that showed differences in amide proton shifts, with the exception of Gly[36] ($\Delta\delta C_\alpha H$ of 0.04 and −0.03 ppm), and were zero for all other residues.

The patterns of shift differences for the (Lys[15]-Val, Pro[13]-Ile) mutant (Figure 4b) are more discernible, although all are again small, i.e., less than 0.2 ppm (contrast this with the overall spread of amide proton resonance in BPTI which ranges from 10.55 to 6.77, some 3.78 ppm). The double mutation causes changes extending over residues 10−20, i.e., the whole binding loop region, and they are enhanced relative to those with the single mutation. Furthermore, changes for the inner-loop region (residues 34−42) are more widespread and of greater magnitude than for the single mutation, and are comparable in size to those of the loop containing the mutations.[2] Amide proton shifts could not be determined for residues Cys[14] and Cys[38], or for Gly[37], as with the single mutant. Once again, changes in shifts for the C_α protons were generally negligible, with the notable exception of Tyr[10] (0.03), Gly[12] (−0.10, −0.10), Arg[17] (0.03), Ile[18] (−0.02), and Gly[36] (0.04, −0.07). Gly[37] and Cys[38] were not observed, as described above. All these changes are for residues adjacent to the sites of mutation.

DISCUSSION

The kinetic data presented in this study show that the specificity of inhibition of BPTI can be altered by the mutation of one or two amino acid residues. The specificities of inhibition of PPE and HLE, by the three BPTI homologues, are similar and significantly different from trypsin. However, the mechanism of inhibition of PPE and HLE

[2] Minor changes are also observed at positions far removed from the sites of mutation, i.e., residues 25 and 49. These can be attributed to the variable N-terminal processing in the *Aspergillus niger* expression system which was used to prepare this mutant (Archer et al., unpublished work). This mutant was not available in sufficient quantity from *E. coli* (Chesshyre et al., 1995) for NMR spectroscopic investigation. Since the N-terminus is close to residues 25 and 49 in the tertiary structure of BPTI, it is not surprising that the additional N-terminal amino acid(s) perturb(s) the NH shifts of these residues. The additional residues were observed in the NMR spectrum, but since the major component was less than 40% of the total protein, their NH shifts have not been incorporated into Figure 4b.

appears to differ, and this may reflect the nature of their active sites. It was assumed initially that the mutations would have relatively little effect on the conformation of the active loop region and the "canonical" interaction (Bode & Huber, 1994) of the BPTI homologues with the serine proteinase would be retained.

The principal determinant for the inhibition of PPE and HLE was demonstrated to be the Lys[15]-Val mutation, i.e., the P_1 residue. Wild-type BPTI, which inhibits trypsin with $K_i = 6 \times 10^{-14}$ M (Lazdunski & Vincent, 1972), does not inhibit PPE (Beckmann et al., 1988) and is a weak inhibitor of HLE (Lestienne & Bieth, 1978). The single mutation completely reverses this inhibition, BPTI (Lys[15]-Val), inhibiting PPE with $K_i = 3 \times 10^{-8}$ M and HLE with $K_i = 2.8 \times 10^{-9}$ M, and does not inhibit trypsin. These results are in reasonable agreement with the work by Beckmann (bearing in mind that the exact conditions were not reported), as well as with work by Courtney on the α_1-proteinase inhibitor with Met at P_1 replaced by Val (Beckmann et al., 1988; Courtney et al., 1986). It was these results that led us to introduce Val at P_1 rather than the oxidatively sensative methionine found in the α_1-proteinase inhibitor. In addition, substrates with Val in the P_1 position are known to be rapidly hydrolyzed by both PPE and HLE (McRae et al., 1980; Nakajima et al., 1979). The amino acids that occupy the P_3 and P_4 sites in the α_1-proteinase inhibitor are Ile and Ala, respectively, which was the reason for incorporating these residues in the double mutants. Cys-14 corresponding to P_2 in the inhibitor could not be changed as this is an essential structural element of BPTI.

Inhibition of PPE by the double mutants, BPTI (Lys[15]-Val, Pro[13]-Ile) and BPTI (Lys[15]-Val, Gly[12]-Ala), showed, through their k_{off} values, that they were less effective inhibitors of PPE; in particular for BPTI (Lys[15]-Val, Gly[12]-Ala), complete dissociation occurs within 5 min. One can conclude, therefore, that PPE tolerates the replacement of the Pro at P_3 by Ile in the active loop of BPTI (Lys[15]-Val, Pro[13]-Ile), but that the replacement of the Gly at P_4 by Ala leads to a significantly less effective inhibitor. By contrast, replacement of Pro at P_3 by Ile in HLE decreases k_{off} and K_i by a factor of 10, but the replacement of Gly by Ala at the P_4 position increases K_i by a factor of 10 and k_{off} by a factor of 5. These mutations had been selected because the α_1-proteinase inhibitor possesses Ile at P_3 and Ala at P_4 (Carrell et al., 1982).

Studies of substrate hydrolysis by PPE and HLE (McRae et al., 1980; Nakajima et al., 1979) suggest that an Ala residue at the P_4 position is accommodated; however; no data appear to be available for a substrate with Gly at P_4 but which is otherwise unchanged. It is interesting to note, therefore, that the double mutant BPTI (Lys[15]-Val, Gly[12]-Ala) is a less effective inhibitor of PPE and a slightly less effective inhibitor of HLE compared with the single mutant BPTI (Lys[15]-Val). Whether this is due to a conformational change in the binding loop or simply that Ala is less well accommodated at the S_4 subsite of these enzymes is not possible to conclude from the kinetic data.

The mutation at the P_3 position (Pro[13]-Ile) has relatively little effect on the inhibition of PPE, but increases the inhibition binding constant for HLE by BPTI (Lys[15]-Val, Pro[13]-Ile). Although a Pro residue it often preferred in the binding loop of protein inhibitors (e.g., for PSTI at P_2, *Streptomyces* subtilisin inhibitor at P_2, Bowman Birk inhibitor at P_3', and α_1-proteinase inhibitor at P_2) (Laskowski & Kato, 1980), it is possible that substitution of the Pro in this case allows the formation of a more favorable loop conformation for the binding to HLE. If this is the case, it seems likely that the retention of the P_2 Cys residue in each of the anti-elastase BPTI mutants is very important for the conformational rigidity of the reactive site loop. The Ile residue improves the interactions with the S_3 subsite. The most effective binding loop sequences in BPTI mutants for the inhibition of PPE and HLE generated from these data are presented in Table 3.

Table 3: Effective Binding Loop Sequences of BPTI Homologues for the Inhibition of PPE and HLE Based on the Data Presented Here

active loop residues	P_4	P_3	P_2	P_1	P_1'
wt BPTI	Gly	Pro	Cys	Lys	Ala
BPTI homologue for HLE	Gly	Ile	Cys	Val	Ala
BPTI homologue for PPE	Gly	Pro	Cys	Val	Ala

The amide NH shift differences observed for the mutant BPTIs compared with the wild-type BPTI are a useful qualitative indicator of the backbone conformational change associated with the mutations. As can be seen from the NH shift differences of all the backbone peptide bonds in BPTI (Lys[15]-Val) (Figure 4a), the mutation only affects resonances up to five residues flanking the site of mutation, but there is also a small effect on the residues of the inner loop, which can be attributed at least in part to transmission through the Cys[14]−Cys[38] disulfide bridge. Lack of NH shift differences for all other residues, and the small magnitude of the changes observed for residues close to the site of mutation, suggests that large conformational changes are not occurring and that the small changes observed are localized around the site of mutation.

The amide NH shift differences from the backbone peptide bonds in BPTI (Lys[15]-Val, Pro[13]-Ile) indicate somewhat larger changes and presumably greater perturbation. Nevertheless, the magnitude of the changes is still small, and they are confined to the inner- and outer-loop regions.[2] The greater changes, especially to residues of the inner loop, are not surprising, since the two mutations flank Cys[14] that forms a disulfide bridge with Cys[38]. Moreover, it is adjacent to two glycine residues (36 and 37) which will facilitate conformational transmission. Although these larger shift differences imply larger conformational changes, the shift differences are still small. Insufficient BPTI (Lys[15]-Val, Gly[12]-Ala) was available for an NMR investigation.

This work suggests that in designing potent protein proteinase inhibitors, it may not be sufficient to "match up" the residues in the active loop of the inhibitor with the known substrate specificity of the enzyme since mutations may also affect the conformation of the active loop of the protein inhibitor. It was initially assumed that the canonical nature of the inhibition of serine proteinases by BPTI would mean that mutations in the active loop would principally affect the specificity of the mutated BPTI and not its conformation. It now seems clear that both will be affected, and that it is not yet possible to predict when the increase in binding energy expected by pairing up inhibitor loop residues with the enzyme specificity will be offset by a decrease in binding

[3] N.B.: For the binding of elafin to HLE, $K_i = 2.0 \times 10^{-10}$ M but $k_{on} = 3.6 \times 10^6$ M^{-1} s^{-1} (Ying & Simon, 1993).

energy arising from a change in the conformation of the active site loop. Nevertheless, it is also clear from this investigation that very potent inhibitors of selected target proteinases can be obtained by mutagenesis of a natural protein proteinase inhibitor.

Both k_{on} and k_{off} are relatively fast for BPTI (Lys[15]-Val) with PPE compared with HLE. This is consistent with the relatively open and accommodating active site of PPE (Bode et al., 1989; Shotton & Watson, 1970). For HLE, the lower K_i values are primarily a reflection of the slower dissociation rate, although the association rate is slower than for PPE due to an isomerization process. Supporting evidence for such an isomerization process (Scheme 1, mechanism B) comes from the crystal structure of the enzyme inhibited with a MeOSucAlaAlaProVal chloromethyl ketone (Wei et al., 1988), the β-branched side of Val being accommodated by a slight tilting of its main chain, leading to shrinking of the S_1 binding pocket. It is therefore possible that the relatively low values for k_{on} reflect this or a similar structural isomerization and do not reflect the rate of encounter of HLE and the BPTI homologues.[3]

REFERENCES

Bax, A., & Davis, D. G. (1985) *J. Magn. Reson. 65*, 355−360.

Beckmann, J., Mehlich, A., Schröder, W., Wenzel, H. R., & Tschesche, H. (1988) *Eur. J. Biochem. 176*, 675−682.

Berndt, K. D., Günthert, P., Orbons, L. P. M., & Würthrich, K. (1992) *J. Mol. Biol. 227*, 757−775.

Bode, W., & Huber, R. (1992) *Eur. J. Biochem. 204*, 433−451.

Bode, W., & Huber, R. (1994) *Fibrinolysis 8*, 161−171, and references cited therein.

Bode, W., Meyer, E., & Powers, J. C. (1989) *Biochemistry 28*, 1951−1963.

Braunschweiler, L., & Ernst, R. R. (1983), *J. Magn. Reson. 53*, 521−528.

Carrell, R. W., Jeppsson, J.-O., Laurell, C.-B., Brennan, S. O., Owen, M. C., Vaughan, L., & Boswell, D. R. (1982) *Nature 298*, 329−334.

Cha, S. (1975) *Biochem. Pharmacol. 24*, 2177−2185.

Chase, T., Jr., & Shaw, E. (1967) *Biochem. Biophys. Res. Commun. 29*, 508−514.

Chen, Z., & Bode, W. (1983) *J. Mol. Biol. 164*, 283−311.

Chesshyre, J. A., Kraunsoe, J. A. E., & Lowe, G. (1995) *Biotechnol. Appl. Biochem. 22*, 269−280.

Courtney, M., Jallat, S., Tessier, L.-H., Crystal, R., & Lecocq, J.-P. (1986) *Philos. Trans. R. Soc. London, A317*, 381−390.

Creighton, T. E. (1992) *Science 256*, 111−112.

Davis, R., & Whittington, R. (1995) *Drugs 49*, 954−983.

Deisenhofer, J., & Steigmann, W. (1975) *Acta Crystallogr. B31*, 238−250.

Fritz, H., & Wunderer, G. (1983) *Arzneim.-Forsch./Drug Res. 33(I)*, 479−494.

Hoult, D. I., Chen, C.-N., Eden, H., & Eden, M. (1983) *J. Magn. Reson. 51*, 110−117.

Huber, R., Kukla, D., Bode, W., Schwager, P., Bartels, K., Deisenhofer, J., & Steigemann, W. (1974) *J. Mol. Biol. 89*, 73−101.

Kassel, B. (1970) *Methods Enzymol. 19*, 844−852.

Largman, C. (1983) *Biochemistry 22*, 3763−3770.

Laskowski, M., Jr., & Kato, I. (1980) *Ann. Rev. Biochem. 49*, 593−626.

Lestienne, P., & Bieth, J. G. (1978) *Arch. Biochem. Biophys. 190*, 358−360.

Lobermann, H., Tokuoka, R., Deisenhofer, J., & Huber, R. (1984) *J. Mol. Biol. 177*, 531−556.

Lomas, D. A., Evans, D. L., Stone, S. R., Chang, W.-S. W., & Carrell, R. W. (1993) *Biochemistry 32*, 500−508.

Longstaff, C., Campbell, A. F., & Fersht, A. R. (1990) *Biochemistry 29*, 7339−7347.

Marion, D., & Bax, A. (1988) *J. Magn. Reson. 79*, 352−356.

McRae, B., Nakjima, K., Travis, J., & Powers, J. C. (1980) *Biochemistry 19*, 3973−3978.

Morrison, J. F., & Walsh, C. T. (1988) *Adv. Enzymol. Relat. Areas Mol. Biol. 61*, 201−301.

Nakajima, K., Powers, J. C., Ashe, B. M., & Zimmerman, M. (1979) *J. Biol. Chem. 254*, 4027−4032.

Rance, M. (1987) *J. Magn. Reson. 74*, 557−564.

Rucker, S. P., & Shaka, A. J. (1989) *Mol. Phys. 68*, 509−517.

Schiffer, C. A., Huber, R., Wüthrich, K., & van Gunsteren, W. F. (1994) *J. Mol. Biol. 241*, 588−599.

Shotton, D. M., & Watson, H. C. (1970) *Nature 225*, 811−816.

Staley, J. P., & Kim, P. S. (1990) *Nature 344*, 685−688.

Tetley, T. D. (1993) *Thorax 48*, 560−565.

Tschesche, H. (1974) *Ang. Chem., Int. Ed. Engl. 13*, 10−28.

Verstraete, M. (1985) *Drugs 29*, 236−261.

Vincent, J.-P., & Lazdunski, M. (1972) *Biochemistry 11*, 2967−2977.

Wagner, G., Braun, W., Havel, T. F., Schaumann, T., Go, N., & Wüthrich, K. (1987) *J. Mol. Biol. 196*, 611−639.

Wei, A.-Z., Mayr, I., & Bode, W. (1988) *FEBS Lett. 234*, 367−373.

Wlodawer, A., Walter, J., Huber, R., & Sjolin, L. (1984) *J. Mol. Biol. 180*, 301−329.

Wlodawer, A., Nachman, J., Gilliland, G. L., Gallagher, W., & Woodward, C. (1987) *J. Mol. Biol. 198*, 469−480.

Ying, Q.-L., & Simon, S. R. (1993) *Biochemistry 32*, 1866−1874.

BI953013B